

# Galaxy formation in pre-processed dark halos

H.J. Mo<sup>1</sup> and Shude Mao<sup>2</sup>  $\star$

<sup>1</sup> *Department of Astronomy, University of Massachusetts, Amherst, MA 01002, USA*

<sup>2</sup> *Jodrell Bank Observatory, Macclesfield, Cheshire SK11 9DL, UK*

## ABSTRACT

Recent  $N$ -body simulations show that the formation of a present-day, galaxy sized dark matter halo in the cold dark matter cosmogony in general consists of an early fast collapse phase, during which the potential associated with a halo is established, followed by a slow accretion phase, during which mass is added rather gently in the outer region. In this paper, we consider the implication of such formation for galaxy formation. We outline a scenario in which the fast collapse phase is accompanied with rapid formation of cold clouds and with starbursts that can eject a large amount of gas from the halo center. The loss of orbital energy of the cold clouds to the dark matter and the ejection of gas from halo center by starburst can significantly reduce the halo concentration. The outflow from the starburst can also heat the gas in the protogalaxy region. Subsequent formation of galaxies in the slow accretion regime is therefore in halos that have been pre-processed by these processes and may have properties different from that given by  $N$ -body simulations. This scenario can help to solve several outstanding problems in the standard  $\Lambda$ CDM model of galaxy formation without compromising its success in allowing structure formation at high redshift. The predicted rotation curves can be significantly flatter than those based on the halo profiles obtained from  $N$ -body simulations, alleviating the discrepancy of the Tully-Fisher relation predicted in the standard  $\Lambda$ CDM model with observations. The flattened galaxy halos allow accreted minihalos to survive in their central regions longer, which may be helpful in producing the flux anomalies observed in some gravitational lensing systems. The preheating by the early starbursts effectively reduces the amount of gas that can be accreted into galaxy halos, which may explain why the baryon fraction in a spiral galaxy is in general much lower than the universal baryon fraction,  $f_B \sim 0.16$ , in the standard  $\Lambda$ CDM model.

**Key words:** galaxies: bulges – galaxies: formation – galaxies: evolution – galaxies: halos – galaxies: starburst – galaxies: interactions

## 1 INTRODUCTION

For many years, the study of galaxy formation has to contend with uncertainties both in cosmology (which determines the spacetime background and initial conditions for structure formation) and in the physical processes that drive evolution. Thanks to recent observations on the Cosmic Microwave Background (CMB) anisotropy and large-scale structure, the cosmological uncertainties are largely resolved, and the study of galaxy formation can now focus on the physical processes. There is now much evidence that we live in a flat universe which is dominated by Cold Dark Matter (CDM), with a total energy density  $\Omega_0 = 1.02 \pm 0.02$ , total matter density  $\Omega_{m,0} = (0.135 \pm 0.009)h^{-2}$ , baryon density  $\Omega_{B,0} = (0.0224 \pm 0.0009)h^{-2}$ , Hubble constant (in units

of  $100 \text{ km s}^{-1} \text{ Mpc}^{-1}$ )  $h = 0.71 \pm 0.04$ , the power-law index of initial perturbation  $n \sim 1$ , and the amplitude of the perturbation power spectrum, as specified by the  $rms$  of the perturbation field smoothed in spheres of a radius  $8 h^{-1} \text{ Mpc}$ ,  $\sigma_8 = 0.85 \pm 0.1$ . The values quoted here are based on the recent results obtained from WMAP observations of the CMB, but are consistent with a large number of other observations (e.g. Spergel et al. 2003). Assuming the density perturbation to be Gaussian, this (small) set of parameters completely determines the CDM model for structure formation. Thus, although the nature of the dark matter and the cosmological constant remains to be explained, there is not much freedom in choosing the spacetime background and initial conditions for galaxy formation.

When combined with a set of standard (simple) assumptions about galaxy formation, this cosmogony has several outstanding problems. First,  $N$ -body simulations have con-

$\star$  E-mail: hjmo@nova.astro.umass.edu; smao@jb.man.ac.uk

stantly shown that dark matter halos in this cosmogony are quite concentrated, which seems to be at odds with the observed rotation curves of dwarf galaxies (e.g. Moore 1994; Burkert 1995; van den Bosch et al. 2000; de Blok, McGaugh & Rubin 2001; Borriello & Salucci 2001; Blais-Ouelette, Amram & Carignan 2001; Dutton et al. 2003) and the observed Tully-Fisher relation for normal disk galaxies (Mo & Mao 2000; Navarro & Steinmetz 2000; van den Bosch et al. 2003). Because of this, alternative models are proposed, where either the dark matter is assumed to be warm or collisional, or the initial power spectrum is assumed to be strongly tilted (e.g. Spergel & Steinhardt 2000; Hogan & Dalcanton 2000; Kamionkowski & Liddle 2000). Although these models may help to reconcile some of the problems outlined above, they are not favored by the recent WMAP result that the formation of the first generation of ionizing sources may have occurred at quite high redshift. The other problem is an old one. When modern CDM dominated theories of galaxy formation were first considered in late seventies (e.g. White & Rees 1978), it was immediately realized that some processes must be invoked to prevent gas from cooling too fast, otherwise all the gas would cool and turn into stars by the present day. Although various feedback schemes have been proposed (Dekel & Silk 1986) to solve this ‘overcooling’ problem, a satisfactory solution remains lacking. In the standard  $\Lambda$ CDM model favored by current observations, the problem is much more severe since the baryon fraction is approximately 16%, which is 3 times higher than that in the standard CDM model with  $\Omega_m = 1$ , making radiative cooling even more effective. The observed baryonic mass fraction in present-day galaxy halos is only a few percent (see §2.3); this poses another serious problem for the present cosmogony, because one has to explain why only such a small fraction of the gas in a protogalactic region eventually assembles into a galaxy. The conventional feedback scheme, where energy feedback from supernova explosions is assumed to drive the cooled gas in a formed galaxy disk out of a galactic halo, may not be a viable solution, because such feedback is only effective in very low mass galaxies (e.g. Mac Low & Ferrara 1999).

The existence of these problems is not necessarily a failure of the standard  $\Lambda$ CDM model because galaxy formation involves many complex physical processes in addition to the cosmological initial and boundary conditions. It is, therefore, possible that we are indeed living in a  $\Lambda$ CDM universe, but that some important pieces of the puzzle are still missing in our current understanding of galaxy formation. In particular, the dynamical role of the baryon component and star formation in structure formation is one important aspect of the problem that has not been fully understood. Since the universal baryon fraction in current cosmogony is quite high and since baryonic gas is dissipational, the baryon component may have played an important role in structure formation, especially on galactic scales. In this paper, we examine the potential of such dynamical effects in solving the problems discussed above.

The scenario we are proposing is motivated by the following considerations. According to recent  $N$ -body simulations (e.g. Wechsler et al. 2002; Zhao et al. 2003a,b), the formation of a galaxy halo in the  $\Lambda$ CDM cosmogony typically consists of two distinct phases: a fast collapse phase during which the gravitational potential associated with a halo is established, and a slow-accretion phase during which

mass is added gently to the halo without significantly affecting the potential well. The early fast-collapse phase is dominated by violent mergers of dark matter halos. Since radiative cooling of gas is very effective in galaxy-sized halos at high redshift (with cooling time much shorter than halo collapse time), this phase is expected to be accompanied by rapid formation of dense gas clouds, which then rapidly collapse into the center of the galaxy halo. During this process, the structure of dark matter halos can be affected by the baryonic component. The violent collapse of the gas clouds in the fast-collapse phase may also trigger an episode of rapid star formation that may drive a large amount of gas out from the halo center. Such mass loss will cause the halo to expand in the inner region, thereby reducing the halo concentration. As we will show below, these two processes combined may be sufficient to overcome the concentration problem in the standard  $\Lambda$ CDM model, given the high baryonic mass fraction in this cosmogony. This early episode of starburst associated with the fast-collapse phase may also heat the gas in a protogalaxy before it collapses, thereby reducing the amount of gas that can be accreted during the slow-accretion phase (e.g. Mo & Mao 2002; Oh & Benson 2003). A proper treatment of these processes is therefore also a key step in understanding the baryon fraction in normal galaxies.

Some of these issues we are considering here have already been discussed in earlier investigations. The importance of the baryon component in affecting halo profile was pointed out in Binney et al. (2001); El-Zant et al. (2001) considered the possibility that the interaction between gas clouds and dark halo can erase the cusps in the halo of dwarf galaxies; Weinberg & Katz (2002) found that the secular evolution of a bar-like structure in a dark matter halo can effectively get rid of the cusps of CDM halos; Navarro et al. (1996) considered the possibility that a sudden blowout of baryons from the center of a dwarf galaxy can cause significant flattening of the inner profile of its halo. The effect of preheating on subsequent gas cooling and galaxy formation has been considered in Mo & Mao (2002) and in Oh & Benson (2003). Our study here intends to present a related discussion in the context of dark halo formation in the current CDM cosmogony, and in particular, we want to demonstrate that a proper treatment of these processes may be pivotal in solving many of the vexing problems in current models of galaxy formation.

This paper is organized as follows. In Section 2 we revisit some of the problems about galaxy formation in the standard  $\Lambda$ CDM model. In Section 3 we examine two possible ways in which the baryon component can affect halo concentration, and we discuss the observational consequences of the change of halo concentrations in Section 4. In Section 5, we examine how an early phase of starburst, which may be responsible for the formation of bulge and halo stars, can affect the subsequent formation of galaxies in dark halos. Finally, in Section 6, we make further discussion about our results.

## 2 SOME OUTSTANDING PROBLEMS OF GALAXY FORMATION IN THE STANDARD $\Lambda$ CDM MODEL

### 2.1 The properties of CDM halos

One important aspect of galaxy formation in the CDM cosmogony is the formation of dark matter halos. Since dark matter particles take part only in gravitational interaction,  $N$ -body simulations can be used to study in detail the formation of dark halos in the cosmic density field, and a great deal has been learned about the properties of the halo population in the past few years. One important finding is that CDM halos can be approximated by a universal profile of the form

$$\rho(r) = \frac{4\rho_s}{(r/r_s)(1+r/r_s)^2}, \quad (1)$$

where  $r_s$  is a scale radius and  $\rho_s$  is the density at this radius (Navarro et al. 1997, hereafter NFW; see Moore et al. 1998, Jing 2000, Klypin et al. 2001 for discussions about the uncertainty of the inner profile). The proper size of a halo is often defined so that the mean density within the halo radius  $r_h$  is a factor  $\Delta_h$  times the mean density of the universe,  $\bar{\rho}$ , at the redshift  $z$  in consideration. The halo mass  $M_h$  is then related to the halo radius by

$$M_h = \frac{4\pi}{3}\bar{\rho}\Delta_h r_h^3. \quad (2)$$

In our discussion we adopt  $\Delta_h = \Delta_{\text{vir}} = (18\pi^2 + 82x - 39x^2)/\Omega_m(z)$ , where  $x = \Omega_m(z) - 1$ , and  $\Omega_m(z)$  is the mass density parameter at redshift  $z$  (Bryan & Norman 1998). For the standard  $\Lambda$ CDM model,  $\Delta_h \approx 340$  at  $z = 0$ . The parameter that characterizes the concentration of mass distribution in a halo is the concentration parameter, defined to be  $c \equiv r_h/r_s$ . It is then easy to show that the total mass within a radius  $r$  is

$$M_h(<r) = M_h f(cx)/f(c), \quad (3)$$

where  $x \equiv r/r_h$ , and

$$f(x) \equiv \ln(1+x) - x/(1+x). \quad (4)$$

The mass within  $r_s$  is

$$M_s = \frac{\ln 2 - 1/2}{f(c)} M_h. \quad (5)$$

Defining the circular velocity of a halo as  $V_h = (GM_h/r_h)^{1/2}$ , we have

$$M_h = \frac{V_h^3}{[\Delta_h \Omega_m(z)/2]^{1/2} G H(z)}, \quad (6)$$

where  $H(z)$  is the Hubble constant at  $z$ . The gravitational potential of the halo at a radius  $r$  from the center is

$$\Phi(r) = -V_h^2 \frac{1}{f(c)} \frac{\ln(1+cx)}{x}, \quad (7)$$

and the escaping velocity is  $V_{\text{esc}}(r) = \sqrt{-2\Phi(r)}$ .

With large  $N$ -body simulations, it is found that the typical value of the concentration depends on halo mass. For the standard  $\Lambda$ CDM model, this mass dependence can be parameterized as

$$c(M) = 11 \left( \frac{M_h}{10^{12} h^{-1} M_\odot} \right)^{0.15} \quad (8)$$

for halos identified at  $z = 0$  (e.g. Bullock et al. 2001; Zhao et al. 2003b). The value of  $c$  also depends on redshift. Numerical simulations show that the concentration of a halo is tightly correlated with its mass accretion history (Wechsler et al. 2002; Zhao et al. 2003a,b). As shown in Zhao et al. (2003a), the formation of each CDM halo in general consists of two phases: a fast collapse phase during which the gravitational potential is established (the formation of the core of potential) and a slow-accretion phase during which mass is gently added to the core of potential without significantly affecting the potential well. The formation of the core of potential is dominated by rapid mergers and halos in this phase have relatively low concentration,  $c \sim 4$ . In the slow-accretion phase, the values of inner quantities, such as  $r_s$ ,  $M_s$  and  $V_s$ , change little, while  $c$  increases as more mass is added in the outer part of the halo. Based on this, one may define a formation time  $t_f$  at which the circular velocity as a function of time remains roughly constant. Zhao et al. found that the formation time defined in this way is closely related to the concentration parameter, and for present-day halos the correlating is well described by

$$c \approx 4 \times \left[ \frac{H(z_f)}{H_0} \right]^{1/\eta}, \quad (9)$$

where  $\eta \sim 1$ . We can invert this relation to write the formation time as a function of  $c$ . For a flat universe, we have

$$1 + z_f \approx \left[ \left( \frac{c}{4} \right)^{2\eta} \frac{H^2(z_f)}{H_0^2} - \Omega_\Lambda \right]^{1/3} \Omega_{m,0}^{-1/3}. \quad (10)$$

For halos of a given mass (or a given circular velocity), the median concentration defines a typical formation time  $t_f$ , while the scatter in  $c$  implies a scatter in  $t_f$ . The median of  $c$  for a  $10^{12} h^{-1} M_\odot$  halo at the present time is about 11, corresponding to a formation redshift  $z_f = 2$ . For a given mass, the dispersion in  $c$  is about 40%, which corresponds to a formation redshift between 1 and 3 for present-day halos with  $M_h \sim 10^{12} h^{-1} M_\odot$ .

### 2.2 The concentration problem

It has been pointed out by several authors that the cuspy NFW halos are at odds with the observed rotation curves of low-surface brightness galaxies, which are fit better by profiles with a constant density core (e.g. de Blok et al. 2001). Even if one enforces the NFW profile in the fit, the obtained concentration parameters are usually much lower than that predicted by the standard  $\Lambda$ CDM model (e.g. Moore 1994; Burkert 1995; van den Bosch et al. 2000; Borriello & Salucci 2001; Blais Ouelette, Amram & Carignan 2001). Although there have been concerns over the effects of beam smearing (van den Bosch et al. 2000; Swaters, Madore & Trewheella 2000), recent analyses of high-resolution  $H\alpha$ -HI rotation curves (de Blok, McGaugh & Rubin 2001; and McGaugh, Barker & de Blok 2002) suggest that the discrepancy appears to be real. Similar problems may exist also for normal spiral galaxies. Matching model predictions with the observed Tully-Fisher relation, Mo & Mao (2000) find that  $c \sim 4$  is required to obtain an agreement. The constraint here comes from the fact that a higher halo concentration leads to a larger boost of the disk maximum rotation velocity

relative to the halo circular velocity, and too high a concentration leads to too low a luminosity for a given maximum rotation velocity. In what follows, we re-visit this problem with the use of more recent data, putting it in the context of our discussions in the present paper.

### 2.2.1 Problem with the Tully-Fisher Relation

Spiral galaxies are observed to show a tight relation between luminosity and rotation velocity  $V_{\text{obs}}$  (which is usually taken to be the maximum rotation velocity). This Tully-Fisher (TF) relation can be written in the form

$$L = AV_{\text{obs}}^\alpha, \quad (11)$$

where  $A$  is the TF amplitude and  $\alpha$  the TF slope. For a given rotation velocity, the observed scatter in  $L$  is quite small, typically about 20% at the bright end.

Theoretically, the mass of a halo with circular velocity  $V_h$  is given by equation (6). If we assume the disk mass is  $M_d = m_d M_h$ , we can write

$$M_d = 9.3 \times 10^{10} h^{-1} M_\odot \left( \frac{m_d}{0.05} \right) \times \left( \frac{V_{\text{obs}}}{200 \text{ km s}^{-1}} \right)^3 \left( \frac{\Delta_h \Omega_{m,0}}{200} \right)^{-1/2} f_V^{-3}, \quad (12)$$

where  $f_V = V_{\text{obs}}/V_h$  is the boost of the observed rotation velocity relative to the circular velocity of the halo. We calculate the boost factor as a function of halo concentration  $c$  and disk mass fraction  $m_d$ , assuming that the halo response to disk formation is through adiabatic contraction (see e.g. Mo, Mao & White 1998 for detailed descriptions). The disk mass can be converted into a disk luminosity by assuming a disk mass-to-light ratio  $\Upsilon_d$ , and so equation (12) can be compared with the observed TF relation, once models for  $\Upsilon_d$  and  $f_V$  are adopted. Since  $f_V$  depends on  $c$ , the observed TF amplitude is a constraint on  $c$ . This is how Mo & Mao (2000) obtained  $c \sim 4$ .

One uncertainty in the predicted TF relation is the adopted mass-to-light ratio, which is assumed to be a constant for a given  $V_{\text{obs}}$  in the model while in reality it may vary from galaxy to galaxy. Thus, a better way to constrain the theoretical model is to use the observed baryon TF relation, which directly relates the mass of cold gas in a spiral galaxy with its rotation velocity  $V_{\text{obs}}$ . Such relation has been obtained by McGaugh et al. (2000) and Bell & de Jong (2002). By modeling in detail the stellar mass and cold gas mass in each galaxy in their sample, Bell & de Jong obtained a baryon mass of  $M_d \approx 7.0 \times 10^{10} M_\odot$  (assuming  $h = 0.71$ ) for galaxies with  $V_{\text{obs}} = 200 \text{ km s}^{-1}$ , which is similar to the value,  $M_d \approx 6.4 \times 10^{10} M_\odot$ , obtained by McGaugh et al. The typical scatter in  $M_d$  at the massive end is about 20%. These observed amplitudes can be compared directly with the prediction given by equation (12), once we know the boost factor  $f_V$  (see e.g. Mo, Mao & White 1998). We also assume disks to have exponential mass profiles and the specific angular momentum is given by a spin parameter  $\lambda = 0.05$ . As shown in Mo et al. (1998), this is the typical spin parameter required to reproduce the observed disk sizes.

Fig. 1 shows the predicted TF amplitude at  $V_{\text{obs}} = 200 \text{ km s}^{-1}$  as a function of  $m_d$  for several values of  $c$ . A comparison with the observational results clearly shows that

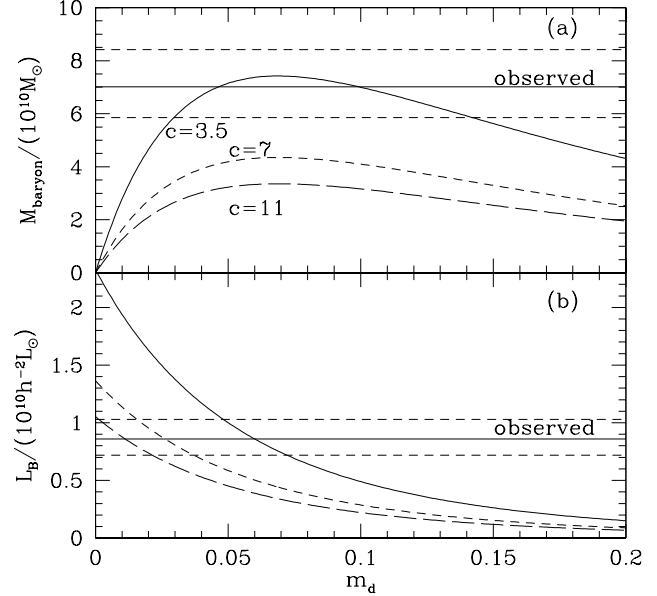


**Figure 1.** (a) The predicted amplitude of the baryon TF relation as a function of  $m_d$  and halo concentration  $c$  (assuming NFW profile) for disk galaxies with  $V_{\text{max}} = 200 \text{ km s}^{-1}$ . The solid horizontal line is the mean value observed by Bell & de Jong (2001), while the two dashed horizontal lines represent 20% deviation from the mean. (b) The predicted amplitude of the  $B$ -band TF relation for  $V_{\text{max}} = 200 \text{ km s}^{-1}$  as required to match the observed luminosity function. The horizontal solid line is the observed amplitude based on Tully & Pearce (2000), while the two dashed horizontal lines represent 20% deviation from the mean.

a low concentration,  $c \lesssim 4$ , is preferred. For  $c = 11$ , the median value for CDM halos in the standard  $\Lambda$ CDM model, the predicted amplitude is lower by a factor of more than two.

Note that even if a low value of  $c$  is adopted, consistency with observation requires  $m_d$  to be substantially smaller than the universal value 0.16. Thus, only a small fraction of baryons in a protogalaxy can manage to settle into the final disk. We will come back to the implication of this result in subsection 2.3.

### 2.2.2 Problem with the Galaxy Luminosity Function

Another constraint on halo concentration can be obtained from the observed luminosity function of galaxies. Detailed modeling of the luminosity function of galaxies in the standard  $\Lambda$ CDM by Yang et al. (2003; see also van den Bosch et al. 2003) shows that the halo mass-to-light ratio is about  $100h$  (in the  $B$ -band) for halos with masses  $M_h \sim 10^{12} h^{-1} M_\odot$  and is higher for both larger and smaller masses. This constraint comes from the fact that the number density of galaxy-sized halos is fixed in the standard  $\Lambda$ CDM cosmology, and so the observed luminosity density in the universe is directly related to the halo mass-to-light ratio. Note that this result of the mass-to-light ratio for galaxy halos is also consistent with the result obtained with gravitational lensing (e.g. Hoekstra, Yee & Gladders 2003). For

a given halo mass-to-light ratio, we can use equation (6) to write the the luminosity of the galaxy hosted by the halo as

$$L_B = 1.86 \times 10^{10} h^{-2} L_\odot \left( \frac{M_h/L_B}{100h} \right)^{-1} f_V^{-3} \times \left( \frac{\Delta_h \Omega_{m,0}}{200} \right)^{-1/2} \left( \frac{V_{\text{obs}}}{200 \text{ km s}^{-1}} \right)^3. \quad (13)$$

This has a form similar to the TF relation, with amplitude depending on the boost factor  $f_V$ . The observed  $B$ -band TF amplitude at  $V_{\text{obs}} = 200 \text{ km s}^{-1}$  is  $8.6 \times 10^9 h^{-2} L_\odot$ . This value is quoted without including dust extinction correction, because such correction is not made in the mass-to-light ratio quoted above (see Yang et al. 2003 for detailed discussion). The constraint given by this relation is shown in the lower panel of Fig. 1. To predict a high enough luminosity with  $c = 11$ , the  $m_d$  is required to be extremely low, but such a low  $m_d$  is not allowed by the baryon TF relation. This inconsistency between the Tully-Fisher zero-point and the luminosity function in the standard  $\Lambda$ CDM model has also been found in almost all semi-analytical models of galaxy formation (e.g. Somerville & Primack 1999; Kauffmann et al. 1999; Benson et al. 2002; Mathis et al. 2002; van den Bosch, Mo & Yang 2003). As one can see from the figure, consistent results can be obtained only when  $c \lesssim 4$ .

### 2.3 Baryon fraction in spiral galaxies

Figure 1 shows that consistency with observation requires  $m_d$  to be much smaller than the universal value 0.16, even if a low value of  $c$  is adopted. Thus, only a small fraction of baryons in a protogalaxy can manage to settle into the final disk. Similar conclusion can be reached from detailed modeling of the mass components in the Milky Way. Based on the kinematics of Galactic satellites and halo objects, the halo mass of the Milky Way is estimated to be about  $2 \times 10^{12} M_\odot$  within a radius of about 200 kpc (Wilkinson & Evans 1999; Sakamoto et al. 2002). The K-band absolute magnitude of the Milky Way obtained by Drimmel & Spergel (2001) is about  $-24.02$ , corresponding to  $8.3 \times 10^{10} L_\odot$ . Assuming  $(M/L)_K \approx 1$  (e.g., Binney & Merrifield 1998), we find a total stellar mass of about  $8.3 \times 10^{10} M_\odot$ . This gives a baryon/total mass ratio of  $\sim 4.2\%$ . A similar number can be obtained from the local baryonic surface density, which is approximately  $50 M_\odot/\text{pc}^2$  (Kulijken & Gilmore 1991). Assuming the Galactic Center is 8 kpc away, and taking a disk scale-length of 2.24 kpc (Drimmel & Spergel 2001), one obtains a mass  $5.6 \times 10^{10} M_\odot$  for the disk. The bulge/disk mass ratio is about 1/5 (Kent et al. 1991), and so the total mass in the bulge and disk is about  $6.7 \times 10^{10} M_\odot$ . This gives a baryon/total mass ratio of  $\sim 3.4\%$ . Since the mass of baryons in other components, such as cold and hot gas, is much smaller, the total baryon fraction in the Milky Way is therefore much smaller than the universal value 16%.

## 3 DYNAMICAL EFFECTS OF THE BARYON COMPONENT

The problems presented above are not necessarily the failure of the standard  $\Lambda$ CDM model because, as mentioned earlier, galaxy formation involves many complex physical processes.

One simple assumption made in the model predictions considered above is that the growth of a galaxy disk in the halo center is a gentle process, so that the gravitational effect of the baryon component can be modeled by adiabatic contraction. This may be a good assumption, at least for halos with cuspy inner profiles, as shown by numerical simulations (e.g. Jesseit, Naab, Burkert 2002). In addition, the model also makes an implicit assumption that the density profiles of dark matter halos, within which disks grow, have the same properties as the halos in cosmological  $N$ -body simulations. This may not be a good assumption if the formation of a galactic halo contains a fast-collapse phase during which the interaction between the baryon component and dark matter can significantly affect the structure of the halo. In this case, the formation of a galaxy disk is in a pre-processed halo that may have properties different from a CDM halo.

Based on this consideration, we propose a scenario of galaxy formation that consists of the following aspects:

- (i) The formation of the core of potential through a fast accretion phase, during which gas cools and collapses to form dense clouds that interact dynamically with dark matter particles;
- (ii) The loss of orbital energy of dense clouds due to dynamical friction against dark matter particles, which increases the kinetic energy of the dark matter in the inner region;
- (iii) A phase of rapid star formation in the fast-accretion phase, which causes the loss of a large amount of gas from the halo center, and causes the inner part of the halo to expand;
- (iv) The heating of the gas in the protogalaxy region by the starburst in the fast accretion phase;
- (v) Subsequent formation of a galaxy disk in the slow accretion phase by cooling of the preheated gas in the pre-processed halo.

In this section we focus on the effect of the baryonic component on the halo.

### 3.1 Collapse of the baryon component and its interaction with dark matter

In the fast collapse phase, i.e. during the formation of the core of potential, the interaction between the gas component and dark matter is a complicated process. If radiative cooling is effective, then gas will cool to form clouds before it collapses in the halo center to form stars. For a completely ionized gas, the cooling time scale can be estimated as

$$t_{\text{cool}} = \frac{3nKT}{2n^2\Lambda(T)}, \quad (14)$$

where  $T$  is the virial temperature of the halo,  $n^2\Lambda(T)$  is the cooling rate per unit volume, and  $n$  is the mean particle density. We use the cooling function given by Sutherland & Dopita (1993) for an ionized gas with metallicity equal to 0.1 times the solar value. This should be compared to the the collapse time

$$t_{\text{coll}} \approx \frac{\pi r_h}{V_h}. \quad (15)$$

For halos with  $t_{\text{cool}} \ll t_{\text{coll}}$ , gas cannot be heated up by the gravitational collapse, while for halos with  $t_{\text{cool}} \gg t_{\text{coll}}$ ,

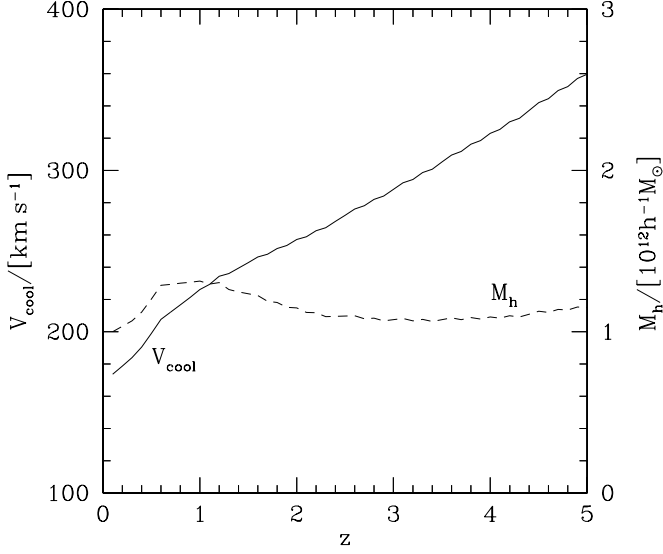


**Figure 2.** The solid curve shows the circular velocity as a function of redshift for halos where cooling time is equal to the collapse time, while the dashed curve shows the masses of such halos. The cooling time uses the cooling function given by Sutherland & Dopita (1993) for an ionized gas with metallicity equal to 0.1 times the solar value.

gas may be heated to the virial temperature and form a hot halo which is approximately in hydrostatic equilibrium in the dark halo potential well. Fig. 2 shows the critical halo circular velocity and mass as a function of redshift, calculated by equating  $t_{\text{cool}}$  and  $t_{\text{coll}}$ . This mass is quite independent of redshift and has a value about  $10^{12} h^{-1} M_{\odot}$ . Thus, in the absence of heating, radiative cooling is effective for halos with masses below that of the Milky Way halo at all redshifts.

We can obtain some ideas about the gravitational interaction between the cold clouds and dark matter particles from numerical simulations of major mergers of galaxies (e.g. Hernquist 1993). In such simulations, each of the merger progenitors is assumed to be a galaxy system consisting of a disk (sometimes a bulge is also included) embedded in an extended dark matter halo. Numerical simulations show that, when two such systems merge, their halos merge first to form a common halo, while the two galaxies lose their orbital energy due to dynamical friction, and sink towards the halo center to merge. Here the dynamical friction plays a key role in the merger of the galaxies. The situation in our problem is more complicated, because the baryon component is still in gaseous form, and so its energy can be dissipated through cloud-cloud collisions. However, simulations of major mergers containing gaseous disks (e.g. Barnes 1992) suggest that such dissipation is important only when the gas clouds have already sunk to the center of the halo, while most of the orbital energy of the cold gas may be lost through dynamical friction. In what follows, we use simple arguments to gain a qualitative understanding of the problem.

According to Chandrasekhar's dynamical friction formula, the dynamical friction force on a gas cloud with mass  $M$  is

$$\mathbf{F}_M = -\frac{4\pi G^2 (\ln \Lambda) \rho_{\text{eff}} M^2}{V_M^3} \mathbf{V}_M, \quad (16)$$

where  $\mathbf{V}_M$  is the velocity of the gas cloud relative to the dark matter,  $\ln \Lambda \sim 10$  is the Coulomb logarithm, and  $\rho_{\text{eff}}$  is the effective mass density of halo particles producing the dynamical friction. The rate at which the gas cloud loses its orbital energy due to dynamical friction is

$$\dot{E} = \mathbf{V}_M \cdot \mathbf{F}_M. \quad (17)$$

For a gas cloud moving in a halo with density profile  $\rho(r)$ , the energy loss rate at radius  $r$  is approximately

$$\dot{E} \propto M^2 \rho(r) / V_M(r). \quad (18)$$

For circular orbits, the decay of the orbital radius is given by

$$\frac{d(rV_M)}{dt} = rF_M/M \propto r\rho M/V_M^2. \quad (19)$$

Assuming that the energy loss of the gas cloud at radius  $r$  is deposited in a spherical shell with radius  $r^\dagger$ , the change in the specific energy of dark matter particles at radius  $r$  is then

$$\mathcal{E} \propto \frac{\dot{E}}{4\pi r^2 \rho(r)} \frac{dt}{dr} \propto \frac{M}{r} \mathcal{G}(r), \quad (20)$$

where

$$\mathcal{G}(r) \equiv \frac{\bar{\rho}(<r)}{\rho(r)} \left[ 1 + \frac{d \ln V_h}{d \ln r} \right],$$

$\bar{\rho}(<r)$  is the mean density of dark matter within radius  $r$ ,  $V_h(r) = [GM_h(<r)/r]^{1/2}$ , and the last relation uses eqs. (18) and (19).

The total energy loss of a cloud is

$$E_{\text{orb}} = \int_0^{r_h} 4\pi r^2 \mathcal{E}(r) dr. \quad (21)$$

For an NFW profile, most of the energy loss is in the inner region, close to  $r = r_s$ , where  $\rho \propto r^{-2}$ . The energy gain per unit mass by the dark matter at radius  $r$  is therefore

$$\mathcal{E} = \mathcal{E}_{\text{orb}} \frac{M}{M_0} \frac{r_s}{r}, \quad (22)$$

where  $\mathcal{E}_{\text{orb}} = E_{\text{orb}}/M$ , and

$$M_0 = \mathcal{G}^{-1}(r) r_s \int_0^{r_h} 4\pi r \rho(r) \mathcal{G}(r) dr. \quad (23)$$

Over a large range of  $r$ ,  $M_0$  is a constant, and  $M_0 \sim M_h$  for an NFW profile with  $c = 4$ .

Assuming isotropic velocity dispersion in a halo, the phase space density profile can be written as

$$Q(r) = \frac{\rho(r)}{[\sigma_i(r)]^3}, \quad (24)$$

where  $\sigma_i(r)$  is the original velocity dispersion at radius  $r$ . As shown by Taylor & Navarro (2001), this phase space density profile can be well approximated by a power law  $Q(r) \propto r^{-1.825}$  for a NFW density profile. If we assume the energy transfer from gas clouds at a radius  $r$  is to be thermalized completely around this radius, the effect on dark matter particles is to increase their velocity dispersion and reduce the phase space density:

<sup>†</sup> This assumption holds only as an average for clouds moving on different orbits.

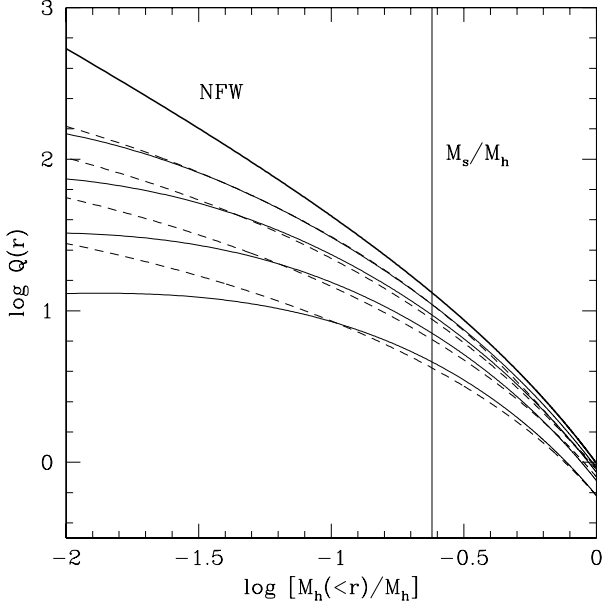


**Figure 3.** The phase-space density profile of dark matter particles. The thick solid curve show that for the NFW profile, while the other solid curves show the profiles taking into account the effect of dynamical friction. Curves from bottom up are results where the gas mass is 0.16, 0.08, 0.04 and 0.02 times the halo mass. The dashed curves show the results for the density profile in eq. (26) assuming  $c' \equiv r_h/r_c = 2.2, 3.5, 5.5, 8.0$  (from bottom up). The values of  $Q$  at the outer radius of the halo are chosen to match those given by the solid curves. The vertical line marks the value of  $M_s$  (cf. eq 5).

$$Q(r) = \frac{\rho(r)}{[\sigma_i^2(r) + \Delta\sigma^2(r)]^{3/2}}, \quad (25)$$

where  $\Delta\sigma(r)$  is the increase in the velocity dispersion due to dynamical friction. Using the expression of  $\mathcal{E}$  to obtain  $\Delta\sigma^2$ , we can obtain the phase-space density profile. Figure 3 show the results for different values of  $f_{\text{gas}} \equiv M_{\text{gas}}/M_h$ , assuming  $c = 4$ . As one can see, the phase-space density in the inner part of the halo can be significantly reduced, and the new phase-space density is roughly a constant in the central region. The effect is larger for a larger value of  $f_{\text{gas}}$ . If  $f_{\text{gas}}$  is comparable to the universal value, 0.16, more than 20% of the dark matter particles will have a roughly constant  $Q$ .

There are a number of uncertainties in the results shown above. First of all, although Chandrasekhar’s formula was shown to describe reasonably well the decay of a satellite’s orbit in a halo of dark matter particles (e.g. Bontekoe & van Albada 1987; Zaritsky & White 1988; Weinberg 1986), the assumption of a local response of the halo may not be valid (e.g. Weinberg 1989; Weinberg & Katz 2002). Because of this, our assumption that the decay of orbital energy of the gas clouds is deposited locally is clearly invalid in detail. Unfortunately, as discussed in Weinberg & Katz (2002), a reliable result of the halo response to sinking satellites is still beyond the capacity of current  $N$ -body simulations, and so the situation remains unclear. We argue, however, that our results are qualitatively correct, because the dark matter

density is the highest in the inner region and so a large fraction of the orbital energy must be deposited there. Furthermore, if the mass fraction in cold clouds is as high as  $\sim 10\%$  of the total halo mass, the orbital energy of the clouds becomes comparable to the total binding energy of the dark matter in the inner region at a radius  $r \sim 0.1r_h$ . Thus, even based on simple energy consideration, the ‘heating’ of dark matter by the cold clouds is expected to be important in the inner region.

### 3.2 Gas outflow and its effect on the halo profile

As the dark matter particles gain energy from gas clouds, the dark halo tends to expand to establish a new equilibrium. On the other hand, the accumulation of gas clouds in the halo center deepens the gravitational potential, which can cause the halo to contract. Which effect dominates depends on the details of the system in consideration. However, the rapid collapse of cold gas in the halo center is likely to be accompanied by rapid star formation, which may drive a large amount of the gas out from the halo center. Observations of nearby starbursts indicate that the mass-loss rate in a system is typically 1 to 5 times the corresponding star formation rate (e.g. Martin 1999). Such mass loss reduces the depth of the potential well, and so the net effect is for the dark halo to expand.

If we assume each mass shell expands adiabatically after the mass loss, we can solve for the density profile from the hydrostatic equilibrium using phase space density profile obtained above. Here, we use a simpler model to demonstrate the basic effect. We assume that the *final* density profile can be described by the form:

$$\rho(r) = \frac{\rho_0 r_c^3}{(r_c + r)^3}, \quad (26)$$

where  $\rho_0$  is the density at the center, and  $r_c$  is a core radius. This profile matches well the NFW profile in the outer region. Assuming isotropic velocity dispersion, the hydrostatic equilibrium equation is

$$\frac{d(\rho\sigma^2)}{dr} = -\rho \frac{GM_h(<r)}{r^2}. \quad (27)$$

Together with the adiabatic equation of state  $\rho/\sigma^3(r) = Q(r)$ , this equation can be integrated to give

$$\frac{Q(r)}{Q_h} = \left(\frac{\rho}{\rho_h}\right)^{5/2} \left[1 + \int_r^{r_h} \frac{\rho(r)}{\rho_h} \frac{V_c^2(r)}{\sigma_h^2} \frac{dr}{r}\right]^{-3/2}, \quad (28)$$

where  $\rho_h$  and  $\sigma_h$  are the density and velocity dispersion at the virial radius, and  $Q_h = \rho_h/\sigma_h^3$ . With the density profile (26), and assuming the value of  $Q_h$  to be the same as that for an NFW profile, we can obtain the phase-space density profile  $Q(r)$ , or  $Q[M_h(<r)]$ . The dashed lines in Fig. 3 show the phase-space density profiles obtained by assuming different values of  $c' \equiv r_h/r_c$ . As one can see, over a large range of mass, the phase space density profiles obtained from §3.1 can be matched by the density profile (26) with appropriate choices of the value of  $c' \equiv r_h/r_c$ . For  $f_{\text{gas}} = 0.16, 0.08, 0.04$ , and  $0.02$ , we obtain  $c' \approx 2.2, 3.5, 5.5$  and  $8.0$ , respectively. Fig. 4 shows the rotation curves given by (26) with these concentrations, as compared with the original NFW profile with  $c = 4$ . Thus, depending on the mass of the gas that can

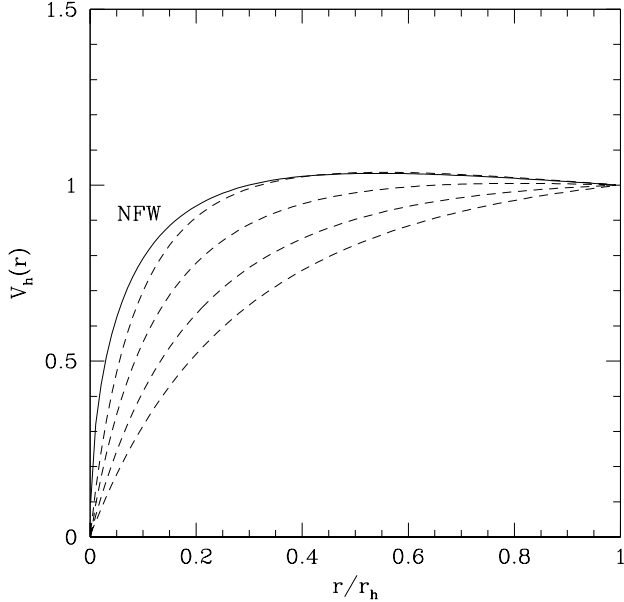


**Figure 4.** The rotation curves of the NFW profile (solid curve) with  $c = 4$  and of the profile (26) with  $c' \equiv r_h/r_c = 2.2, 3.5, 5.5, 8.0$  (from bottom up). The rotation velocity is in units of  $V_h$  while the radius is in units of  $r_h$ .

collapse into the halo center and ejected by galaxy wind, the resulting rotation curve can be flattened substantially relative to that given by the original NFW profile.

## 4 OBSERVATIONAL CONSEQUENCES

### 4.1 The Tully-Fisher relation

In the slow accretion phase after the formation of the core of potential, the virial radius increase roughly as  $H^{-1}(z)$  without affecting much the inner structure. The halo concentration will then increase by a factor of about  $H(z_f)/H_0$  from the formation time to the present time. For galaxy halos with typical formation redshift  $\sim 2$ , this is a factor of 2 to 3. Thus, for a pre-processed halo with concentration  $c' \sim 3.5$  at formation, the concentration at the present time will be between 7 and 10. As shown in Mo & Mao (2000), disk galaxies formed in halos with profile (26) and with such concentrations can match the observed Tully-Fisher relation. Thus the flattening of dark matter halos in the fast collapse phase by the baryon component can help to reconcile the standard  $\Lambda$ CDM model with the observed Tully-Fisher relation.

### 4.2 Dark matter in galaxies

The concentration of galaxy halos can be studied by looking at the fraction of dark matter mass in galaxies. The mass in the central parts of galaxies are expected to be more dominated by dark matter, if dark halos have higher concentrations, and vice versa. Since the total mass can be inferred from observations of kinematics, while the contribution from stars and gas can be inferred by other means, it is possible to infer what fraction of the gravitational mass is in dark matter. For spiral galaxies, this can be done by modeling

the rotation curves and the stellar mass distribution in detail. The results are not yet conclusive (see e.g. Bosma 1998 and references therein). The rotation curves for some bright spirals are observed to decrease just beyond their optical radius, which is best explained if the mass in the central region is dominated by the stellar component (e.g. Noordermeer et al. 2003). On the other hand, there are also spiral galaxies, whose rotation curves are quite flat around the optical radius (e.g. Dutton et al. 2003). The rotation curves of many bright spiral galaxies can be fitted by the maximal disk model, in which the inner rotation curve is assumed to be completely dominated by the stellar components. Although this does not mean that real spirals all have maximal disks, it does suggest that the inner rotation curves of some bright galaxies may be dominated by the stellar component. Similar constraints may be obtained from the fact that the bars in some spiral galaxies are rotating fast. This is not expected if the central region of a barred galaxy were dominated by dark matter, because the bar rotation would be slowed down rather rapidly by the dynamical friction of the dark matter (e.g. Weinberg 1985; Debattista & Sellwood 2000; Weiner, Sellwood & Williams 2001). All these observations suggest that some spirals are dominated by the stellar component in their inner regions.

If the halos of spiral galaxies are as concentrated as CDM halos given by  $N$ -body simulations, most spiral galaxies will be dominated by dark matter, unless the disk is unreasonably heavy (e.g. Mo, Mao & White 1998). On the other hand, for a pre-processed halo with an extended core, the contribution from dark halo is significantly reduced, making it more likely to observe spirals with inner rotation curves dominated by stellar mass.

For elliptical galaxies with moderate luminosities ( $L \sim L_*$ ), recent observations based on the kinematics of planetary nebulae show that the observed velocity dispersion profiles up to  $\sim 5$  effective radii are consistent with being totally due to stellar mass (Romanowsky et al. 2003), indicating the presence of little or no dark matter at these radii. As discussed by these authors, this result is difficult to understand if these galaxies possess dark halos with properties similar to those of the CDM halos. However, if the formation of these galaxies is similar to that of the bulges of spiral galaxies, their halos may be significantly flattened by the processes envisaged in this paper. In this case, the observational result may be easier to understand with the standard  $\Lambda$ CDM model.

### 4.3 Survival of substructures in the halo

After the formation of the core of potential, halo will continue to accrete mass in the form of small halos. High-resolution  $N$ -body simulations show that some of the accreted halos can survive as subhalos (e.g. Klypin et al. 1999; Moore et al. 1999; De Lucia et al. 2003). Intriguingly, the predicted number of sub-haloes in CDM exceeds the observed number of *luminous* satellite galaxies in a Milky-Way type galaxy. One solution for this crisis may be that some of the subhalos, especially those of lowest mass, do not form many stars and hence remain dark. One of the best ways to detect such substructures is through gravitational lensing. The ‘‘anomalous’’ flux ratios in gravitational lenses are

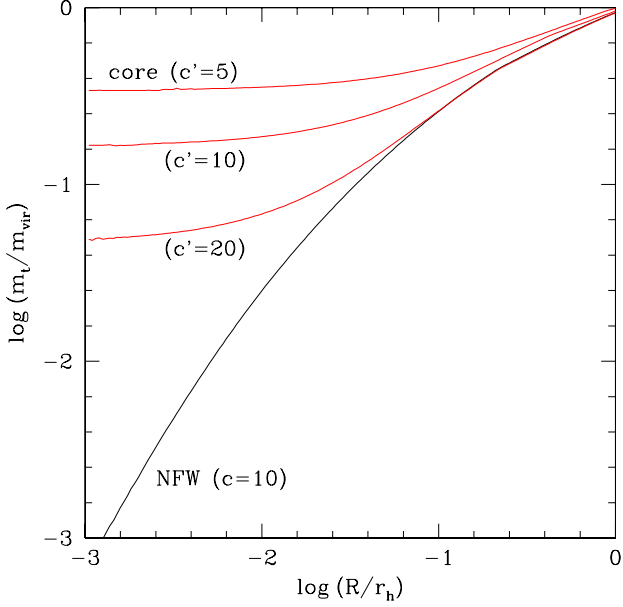


**Figure 5.** The ratio between the mass within the tidal radius and the original virial mass for a small halo (approximated by an NFW profile with  $c = 20$ ) at a given distance from the center of a large halo. The large halo is either assumed to have a NFW profile with  $c = 10$ , or has the profile given by (26), with  $c' \equiv r_h/r_c = 5, 10, \text{ and } 20$ , respectively.

thought to be evidence for substructures (e.g. Mao & Schneider 1998; Kochanek & Dalal 2003 and references therein).

In an NFW halo, most of the subhalos are distributed in the outer part, because subhalos can be destroyed by tidal disruption in the inner part. The situation is different in our scenario, where subhalos may exist in the central part of a galaxy halo because of the reduced tidal effect in the extended core.

Consider the accretion of a minihalo with circular velocity  $\sim 30 \text{ km s}^{-1}$  by a galaxy halo with a circular velocity of  $200 \text{ km s}^{-1}$ . In the presence of a strong UV background, minihalos are not expected to trap gas to form stars (e.g. Gnedin 2000), and so their density profiles are not altered significantly by the interaction with the baryonic component. If such halos can be approximated as NFW profiles, then according to equation (8), they will have a typical concentration  $c \sim 20$ . We calculate the tidal radius of such a minihalo in a galaxy halo with or without a core. The tidal radius,  $r_t$ , of a minihalo with mass  $m$  moving at a radius  $R$  from the center of a large halo with mass  $M$  is the minimum of the following two radii: (1) a radius at which the gravity of the small halo is equal to the tidal force of the big halo, and (2) a radius defined by the resonances between the force the minihalo exerts on the particle and the tidal force by the large halo (e.g. Klypin et al. 1999). The first radius can be solved from

$$\left(\frac{R}{r_t}\right)^3 \frac{m(r_t)}{M(R)} = 2 - \frac{R}{M(R)} \frac{\partial M}{\partial R}, \quad (29)$$

where  $M(R)$  is the mass within radius  $R$ . The second radius, assuming primary resonance, is given by  $\Omega(r)|_{\text{small}} =$

$\Omega(R)|_{\text{large}}$ , where  $\Omega$  is the angular speed. Fig. 5 shows the mass a minihalo can retain within the tidal radius as a function of the distance to the center of the big halo. Results are shown for cases where the large halo either has a NFW profile with  $c = 10$ , or has the profile given by (26) with  $r_h/r_c = 5, 10, \text{ and } 20$ , respectively. If the halo has a core with  $c' \equiv r_h/r_c$  as small as 10, as is required to match the Tully-Fisher relation, a minihalo can retain more than 20% of its original mass, in strong contrast with the case where the host halo has the original NFW profile. This clearly demonstrates that the survival of subhaloes in the central part of galaxies is likely to be sensitive to the inner mass profiles. Note, however, that in Fig. 5, we have neglected the effect of baryons which may steepen the central density profiles and hence destroy some subhaloes. It is currently unclear what might be the eventual survival fraction of subhaloes in a realistic galaxy.

## 5 PREHEATING AND GALAXY FORMATION

### 5.1 Preheating of a protogalaxy region

In order for the starburst in the core of potential to eject large amount of gas from the dark halo potential well, sufficient number of stars must form so that the kinetic energy from supernova explosions from massive stars can heat the gas to a temperature comparable to the escape temperature. For an NFW profile, the escape velocity can be calculated from equation (7). We obtain

$$V_{\text{esc}}(0) = \sqrt{-2\Phi(0)} = \beta V_h, \quad (30)$$

where  $\beta \sim 3.1$  and  $3.7$  for  $c = 4$  and  $10$ , respectively. We write the star formation rate as

$$\dot{M}_* = \frac{M_{\text{gas}}}{\tau t_{\text{ff}}}, \quad (31)$$

where  $M_{\text{gas}}$  is the total mass of cold gas that has assembled in the halo center in the fast accretion phase,  $t_{\text{ff}}$  is the free-fall time of the gas, and  $\tau$  is a constant. The total mass of stars that can form can be written as

$$M_* = \dot{M}_* t_* = M_{\text{gas}} \epsilon_*, \quad (32)$$

where  $t_*$  is the star formation time, and  $\epsilon_* \equiv t_*/(\tau t_{\text{ff}})$  is the star formation efficiency. The total kinetic energy from Type II supernova explosions can be written as

$$E_{\text{sn}} = M_* \nu \epsilon_{\text{sn}}, \quad (33)$$

where  $\nu$  is the number of supernovae per unit mass, and  $\epsilon_{\text{sn}}$  is the kinetic energy per supernova. We adopt  $\epsilon_{\text{sn}} = 10^{51} \text{ erg}$  and  $\nu = (125 M_\odot)^{-1}$ . The value of  $\nu$  quoted here assumes a Salpeter initial mass function (with a lower cutoff of  $0.1 M_\odot$  and an upper cutoff of  $100 M_\odot$ ). If a fraction of  $\epsilon_0$  of this energy is to heat the gas, the specific thermal energy of the gas will be

$$\mathcal{E} = \frac{\epsilon_0 E_{\text{sn}}}{M_{\text{gas}}} = \epsilon_0 \nu \epsilon_{\text{sn}} \epsilon_* \approx (630 \text{ km s}^{-1})^2 \epsilon_0 \epsilon_*. \quad (34)$$

Requiring this specific energy to be equal to the escape temperature, we obtain the star formation efficiency,

$$\epsilon_* = \left(\frac{\beta V_h}{630 \text{ km s}^{-1}}\right)^2 \epsilon_0^{-1}. \quad (35)$$

Note that this relation is meaningful only when  $\epsilon_* < 1$ , and so it only applies for halos with circular velocities smaller than  $\epsilon_0^{1/2}\beta^{-1}630 \text{ km s}^{-1}$ . For larger halos, all cooled gas can form stars and so  $\epsilon_* \sim 1$ . This scaling relation between star formation efficiency and halo circular velocity is similar to that obtained by Dekel & Silk (1986) based on a calculation of supernova remnants in a uniform medium, and has been extensively used in semi-analytic models of galaxy formation (e.g. White & Frenk 1991). The value of  $\epsilon_0$  obtained by Dekel and Silk is about 0.02. Since  $\epsilon_*$  must be smaller than 1, this low value of  $\epsilon_0$  implies that wind can only escape in small halos, with  $V_h \lesssim 30 \text{ km s}^{-1}$  (assuming  $\beta = 3$ ). On the other hand, observations of supernova-driven wind in starburst galaxies require much higher efficiency. The observations of superwind in local starburst galaxies suggest that most of the supernova energy is contained in the superwind (Heckman et al. 2000). Such high efficiency may be more relevant to our discussion, as we are mainly concerned with starbursts. In this case, wind can escape from halos with circular velocities as high as  $200 \text{ km s}^{-1}$ . In principle, the effective value of  $\epsilon_0$  can be larger than 1, if active galaxy nuclei associated with starbursts also contribute to the heating.

The gas that has been heated up to the escaping temperature will escape the core of potential on a time scale  $t_{\text{esc}} \sim r_{\text{cp}}/V_{\text{esc}} \lesssim 1/[10\beta H(z_f)]$ , where  $r_{\text{cp}}$  is the radius of the core of potential, and  $H(z_f)$  is the Hubble constant at the redshift  $z_f$  when the core of potential was formed. This time scale is shorter than the time scale for mass accretion in the slow accretion phase, which is typically the age of the universe. Thus, the out-going wind will interact with the gas outside the core of potential before the gas is accreted by the potential well. The average overdensity within a region that will eventually form a halo at the present time is  $\delta(z_f) = \delta_c/D(z_f)$ , where  $\delta_c \sim 1.68$  is the critical linear overdensity for spherical collapse, and  $D(z_f)$  is the linear growth factor at  $z_f$ . For a flat universe with  $\Omega_{\text{m},0} = 0.3$  we have  $\delta(z_f) \approx 0.43, 0.53, 0.71, 1.03$  for  $z_f = 4, 3, 2$  and 1, respectively. Thus, for halos with an early formation time, the overdensity around the core of potential is moderate at  $z_f$ . Based on the extended Press-Schechter formalism (Bond et al. 1991), one can show that, in the standard  $\Lambda$ CDM model, more than half of the mass of a present galaxy-sized halo was in progenitors with circular velocities  $\lesssim 50 \text{ km s}^{-1}$  at redshift  $z = 2 - 3$ . Such progenitors can retain only a small fraction of their gas either because their potentials are too shallow to trap gas heated by photoionization, or because supernova explosions in themselves or from nearby galaxies can effectively expel the gas (e.g. Scannapieco, Ferrara & Broadhurst 2000). Thus, at the formation redshift of a present-day galaxy halo, most of the mass that is not in the core of potential is in halos that cannot trap much gas. Thus, the wind generated in the core of potential by starburst will be propagating in a relatively uniform medium.

Because the gas density in the post shock medium is in general quite low and so radiative cooling of the shocked gas is negligible, we may use the wind solution of Weaver et al. (1977) (which assumes a constant energy injection rate and neglects radiative cooling and galaxy potential) to get some idea about how much gas can be affected by the wind. In this case, the radius of the shock front changes with time as

$$R_s \sim \left(\frac{125}{154\pi}\right)^{1/5} \left(\frac{E\Delta t^2}{\rho}\right)^{1/5}, \quad (36)$$

where  $E$  is the total supernova energy,  $\rho$  is the gas density of the medium, and  $\Delta t$  is the propagation time. Inserting  $E = (1/2)M_{\text{wind}}\beta^2 V_h^2$  into the above expression, and using the relations between  $M_h$ ,  $r_h$  and  $V_h$ , we obtain

$$R_s \sim 10r_h \left(\frac{\Delta t}{t_f}\right)^{2/5} \left[\frac{f_{\text{wind}}\beta^2}{9}\right]^{1/5}, \quad (37)$$

where  $t_f \approx 1/H(z)$  is the age of the universe when the starburst is generated, which is set to equal the formation time of the core of potential, and  $f_{\text{wind}}$  is the gas mass fraction in the wind. This radius corresponds to a mass  $M \sim (1000/\Delta_h)(\Delta t/t_f)^{6/5} M_h$ , where  $M_h$  is the mass of the core of potential, i.e. the mass of the halo at the formation time. Thus, within a Hubble time, the wind can affect a large volume around the halo. For a halo that formed at a redshift  $z_f$  with circular velocity  $V_h$  and concentration  $c$ , the total mass at the present time is about  $H(z_f)/H_0$  times the progenitor mass. Thus, for a halo formed at  $z \sim 3$ , all the gas in the halo proper can be affected by the wind generated in the core of potential, if the star formation efficiency is as high as discussed above.

Unfortunately, the details about the interaction between the outgoing winds and the intergalactic medium are very complicated, and we are not able to make a detailed discussion here. If we assume that half of the energy of the wind is thermalized in the protogalaxy region, then the specific thermal energy gained by the gas is

$$\mathcal{E} = [H_0/H(z_f)](\beta V_h)^2/4. \quad (38)$$

The corresponding specific entropy of the gas is

$$\begin{aligned} \mathcal{S} &\equiv \frac{T}{n^{2/3}} = \frac{[H_0/H(z_f)]f_{\text{wind}}(\beta V_h)^2}{4[\bar{n}(z_f)(1+\delta_f)]^{2/3}} \\ &\sim 8.5 \times 10^2 \text{ keV cm}^2 \frac{[H_0/H(z_f)]}{(1+z_f)^2(1+\delta_f)^{2/3}} \\ &\quad \times \left(\frac{f_{\text{wind}}^{1/2}\beta V_h}{200 \text{ km s}^{-1}}\right)^2 \end{aligned} \quad (39)$$

where  $\bar{n}(z_f)$  is the mean gas density of the universe at  $z_f$ , and  $\delta_f$  is the overdensity of the protogalaxy region. Thus, in terms of the value of  $\mathcal{S}$ , heating is more effective for halos with higher  $V_h$  and lower  $z_f$ . Taking  $z_f = 3$ ,  $\delta_f = 1$ , and  $\beta = 3$ , we have  $\mathcal{S} \sim 75(V_h/200 \text{ km s}^{-1})^2 \text{ keV cm}^2$ . This should be compared with the characteristic specific entropy of the gas in a virialized halo:  $S_v = T_v/n_v^{2/3} \sim 70 \text{ keV cm}^2 (V_h/200 \text{ km s}^{-1})^2/(1+z)^2$ . Note that both  $\mathcal{S}$  and  $S_v$  scale with  $V_h$  in a similar way, and  $\mathcal{S} \gtrsim S_v$  at all  $z \gtrsim 0$ . Thus the heating from the core of potential can have an important impact on the subsequent collapse of the gas into galaxy halos.

## 5.2 Formation of disk galaxies

In the scenario we are considering here, it is quite natural to associate the formation of galaxy bulges with the fast collapse phase. Depending on whether a significant disk can grow in the subsequent slow accretion phase, a spiral galaxy with some disk/bulge ratio will form. Since the efficiency

of gas cooling is reduced in a preheated gas, the amount of gas that can eventually form a disk can be much lower than that implied by the universal baryon fraction (see Mo & Mao 2002 for details). Also, the bulge/disk ratio is expected to depend on environment, because galaxy halos in high density regions may not be able to accrete much gas before they merge into large systems where radiative cooling is no longer effective. As pointed out in Mo & Mao (2002), this may be responsible for the observed morphology segregations of galaxies. In what follows, we consider several other factors that may have played important roles in determining the morphological types of galaxies.

As shown by equation (35), the star formation efficiency in the fast collapse phase is likely to be more efficient in halos with higher circular velocity. This effect alone would mean that bulges are more important in systems with larger  $V_h$  (or mass). This is consistent with the observational trend that later type galaxies generally have lower luminosities (e.g. Roberts & Haynes 1994). In addition to this mass sequence, halo formation history may also play a role in determining the bulge-to-disk ratio of the galaxy that forms in the halo. Although halos of a given mass have a typical formation time, the dispersion among different halos is large for low-mass halos, and so there are significant number of present-day galaxy halos that can have their cores of potential formed only recently (e.g. Zhao et al., 2003b). Such halos in general have low concentration, as discussed above, but higher specific angular momentum (e.g. Maller, Dekel & Somerville 2002). Gas accretion history by such halos is expected to be different from that for a halo with early formation. First, because of the late formation, the gas associated with the region that eventually collapses to form the core of potential may have already been heated up by star formation in small progenitors before the formation of the core of potential. Second, since the characteristic density is lower at lower redshift, cooling is less effective at the formation time for a later formation. Thus, the formation of the core of potential of such halos is not expected to be associated with rapid formation of cold clouds and with strong starburst. Such systems are therefore expected to have small bulges and may be identified as late-type galaxies. The halos of such galaxies are therefore expected to have lower concentration, and the inner profiles of their halos are expected to be less affected by the bulge formation. Because of the late formation, these systems are expected to show weaker clustering than normal galaxies (e.g. Mo & White 1996). The latter prediction is consistent with the observations that late-type galaxies, such as low surface-brightness galaxies, have weaker correlation in space than average spiral galaxies (e.g. Mo, McGaugh & Bothun 1994).

An interesting question here is whether there are truly bulgeless galaxies. The halos of such galaxies should not have been pre-processed by the bulge formation and so should preserve their original profile. Any bulgeless galaxies with halos that contain extended cores should therefore be considered as serious evidence against the CDM cosmogony. As mentioned earlier, the rotation curves of many low surface-brightness galaxies are better fit with halo profiles with cores. Whether or not all these galaxies have a significant bulge component is still a question of debate. Giant bright low surface-brightness (LSB) disk galaxies such as MALIN-1 are known to have normal bulges (e.g. Bothun, Impey &

McGaugh 1997) and so their halos are expected to be significantly pre-processed. Early observations in blue bands show that many low-luminosity LSBs are bulgeless (see Bothun et al. 1997), but recent observations of such galaxies in near infrared bands suggest that many of them have detectable bulges in old stars and show episodic star formation (e.g. Galaz et al. 2003). Since these galaxies are associated with shallow potential wells, the implied amount of early star formation may be significant in driving large amount of gas out from halo center, thereby altering the inner profiles of their halos. Clearly, detailed modeling is required in order to show if the scenario we are proposing here is consistent with this population of galaxies.

## 6 DISCUSSION

We have outlined a scenario of galaxy formation in which the host halos of present-day galaxies may be significantly flattened in the inner region by interaction with the gas component in an early phase of rapid collapse accompanied by starburst. Our scenario is based on recent simulation results that such a phase is expected in the current  $\Lambda$ CDM model of structure formation. We have shown that this scenario can help to alleviate several vexing problems in current theory of galaxy formation.

Much further work is required to make quantitative predictions with the scenario we have proposed. For example, the treatment of dynamical friction is performed in an oversimplified manner. In order to model this process quantitatively, high-resolution numerical simulations are required. In addition, the assumption of adiabatic contraction should be more carefully checked, particularly for cored halo profiles (such as that described by eq. 26). Ideally, we should use cosmological simulations that fully account for all the relevant processes, such as gas cooling, cloud formation, star formation, outflow and dynamical friction. Unfortunately, such simulations are not yet feasible at the present time. A more realistic approach is to tackle the problem step by step. For example, the dynamical friction may be studied using high-resolution  $N$ -body simulations where cold clouds are represented by simple  $N$ -body systems; the interaction between the starburst-driven wind and the protogalaxy gas may be studied using controlled simulations of individual systems. We intend to return to some of these issues in future papers.

## REFERENCES

- Barnes J.E., 1992, ApJ, 393, 484
- Bell E.F.; de Jong R. S., 2001, ApJ, 550, 212
- Benson A.J., Lacey C.G., Baugh C.M., Cole S., Frenk C.S., 2002, MNRAS, 333, 156
- Binney J., Gerhard O., Silk J., 2001, MNRAS, 321, 471
- Binney J., Merrifield M. 1998, Galactic Dynamics, p. 662 (Princeton: Princeton University Press)
- Blais-Ouellette S., Amram P., Carignan C., 2001, AJ, 121, 1952
- Bond J. R., Cole S., Efstathiou G., Kaiser N., 1991, ApJ, 379, 440
- Bontekoe T.R., van Albada T. S., 1987, MNRAS, 224, 349
- Bothun G., Impey C., McGaugh S., 1997, PASP, 109, 745
- Bryan G.L. & Norman M., 1998, ApJ, 495, 80

- Bullock J. S., Kolatt T. S., Sigad Y., Somerville R. S., Kravtsov A. V., Klypin A. A., Primack J. R., & Dekel A. 2001, MNRAS, 321, 559
- de Blok W.J.G., McGaugh S.S., Bosma A., Rubin V.C., 2001, ApJ, 552, L23
- Dekel A., Silk J., 1986, ApJ, 303, 39
- De Lucia G., Kauffmann G., Springel V., White S.D.M., 2003, astro-ph/0306205, submitted to MNRAS
- Dutton A.A., Courteau S., Carignan C., de Jong R., 2003, astro-ph/0310001
- El-Zant A., Shlosman I., Hoffman Y., 2001, ApJ, 560, 636
- Galaz G., Dalcanton J.J., Infante L., Treister E., 2003, AJ, 124, 1360
- Gnedin, N.Y., 2000, ApJ, 542, 535
- Heckman, T.M.; Lehnert, M. D.; Strickland, D. K.; Armus, L., 2000, ApJS, 129, 493
- Hernquist, L., 1993, ApJS, 86, 389
- Hoekstra H., Yee H.K.C., Gladders M.D., 2003, astro-ph/0306515, submitted to ApJ
- Hogan C., Dalcanton J.J., 2000, Phys. Rev. D62, f3511
- Jesseit R., Naab T., Burkert A., 2002, ApJ, 571, L89
- Kaiser, N., 1991, ApJ, 383, 104
- Kamionkowski M., Liddle A.R., 2000, Phys. Rev. Lett., 84, 4525
- Kauffmann G., Colberg J.M., Diaferio A., White S.D.M., 1999, MNRAS, 303, 188
- Kent, S.M.; Dame, T.M.; Fazio, G., 1991, ApJ, 378, 131
- Kochanek, C.S., Dalal, N. 2003, preprint (astro-ph/0302036)
- Jing, Y. P. 2000, ApJ, 535, 30
- Klypin A.A., Gottloeber S., Kravtsov A.V., Khokhlov A.M., 1999, ApJ, 516, 530
- Klypin A.A., Kravtsov, A. V., Bullock, J. S., & Primack, J. R. 2001, ApJ, 554, 903
- Mac Low, M-M, Ferrara A., 1999, ApJ, 513, 142
- Maller A.H., Dekel A., Somerville R., 2002, MNRAS, 329, 423
- Mao, S., Schneider, P. 1998, MNRAS, 295, 587
- Martin C.L., 1999, ApJ, 513, 156
- Mathis H., Lemson G., Springel V., Kauffmann G., White S.D.M., Eldar A., Dekel A., 2002, MNRAS, 333, 739
- McGaugh, S. S.; Schombert, J. M.; Bothun, G. D.; de Blok, W. J. G., 2000, ApJ, 533, L99
- Mihos J. C.; Dubinski J., Hernquist L., 1998, ApJ, 494, 183
- Mo H.J., Mao S., 2000, MNRAS, 318, 163
- Mo H.J., Mao S., 2002, MNRAS, 333, 768
- Mo H.J., Mao S., White S.D.M., 1998, MNRAS, 295, 319 (MMW)
- Mo H.J., McGaugh S.S., Bothun G. D., 1994, MNRAS, 267, 129
- Mo H.J., White S.D.M., 1996, MNRAS, 282, 347
- Navarro J.F., Eke V.R., Frenk C.S. 1996, MNRAS, 283, L72
- Navarro, J. F., Frenk, C. S., & White, S. D. M. 1997, ApJ, 490, 493
- Noordermeer E., van der Hulst J.M., Sancisi R., Swaters R.A., 2003, astro-ph/0310868
- Oh S.P., Benson A.J., 2003, MNRAS, 342, 664
- Roberts M.S., Haynes M.P., 1994, ARA&A, 32, 115
- Romanowsky A.J. et al. 2003, astro-ph/0308518
- Sakamoto, T.; Chiba, M.; Beers, T.C., 2002, astro-ph/0210508, A&A in press
- Somerville R.S., Primack J.R., 1999, MNRAS, 310, 1087
- Spergel D.N., Steinhardt P. 2000, Phys. Rev. Lett, 84, 3760
- Spergel D.N. et al, 2003, astro-ph/0302209
- Sutherland R.S., Dopita M.A., 1993, ApJS, 88, 253
- Taylor J.E., Navarro J.F., 2001, ApJ, 563, 483
- Tully R.B., Pierce M.J., 2000, ApJ, 533, 744
- van den Bosch, F.C., Mo H.J., Yang X., 2003a, MNRAS, in press
- van den Bosch, F.C., Yang X., Mo H.J., 2003b, MNRAS, 340, 771
- Wechsler R. H., Bullock J. S., Primack J. R., Kravtsov A. V. & Dekel A., 2002, ApJ, 568, 52
- Weinberg M.D., 1986, ApJ, 300, 93
- Weinberg M.D., 1989, MNRAS, 239, 549
- Weinberg M.D., Katz N., 2002, ApJ, 580, 627
- Weiner B.J., Sellwood J.A., Williams T.B., 2001, ApJ, 546, 931
- White S.D.M., Frenk C.S., 1991, apj, 379, 52
- White S.D.M., Rees M.J., 1978, MNRAS, 183, 341
- Wilkinson, M.I., Evans N.W., 1999, MNRAS, 310, 645
- Yang X., Mo H.J., van den Bosch F.C., 2003, MNRAS, 339, 1057
- Zaritsky D., White S.D.M., 1988, MNRAS, 235, 289
- Zhao D.H., Mo H.J., Jing Y. P., & Boerner G., 2003a, MNRAS, 339, 127
- Zhao D. H., Jing Y. P., Mo H.J. & Boerner G., 2003b, ApJ, 597, L9